Blurring the line between intrinsic and scattering attenuation by means of the Shannon entropy

Kris Innanen

ABSTRACT

We compute a version of the Shannon entropy S of snapshots of a seismic wave field as it propagates. S is argued to be a measure of the degree of either multiple scattering, or attenuation, or both, experienced by the wave, evolving similarly regardless of which process dominates in a given example. Invoking it, therefore, forces us to reject the distinction between intrinsic and extrinsic attenuation, and allows us to place thin-bed reverberations above and below the resolving power of the experiment on an equal footing should we decide to do so. S is easily computable, as is shown with both synthetic ("wave in a box") examples and a field VSP example. It relies on stable estimates of the histograms of wave amplitude values, and the best way of doing this is still under investigation.

INTRODUCTION

Since the paper of O'Doherty and Anstey (1971), a good deal of attention has been paid to the ability of two distinct physical mechanisms, scattering and intrinsic friction, to generate the same measurable phenomenon—seismic attenuation. The "OA" view is of a coherent, organized wave pulse being persistently exposed to processes of multiple reflection, occurring on spatial scales below that of the wavelet, acting to cause disorder within it. This manifests as phase and amplitude changes that are indistinguishable from those due to anelastic attenuation, in which wave energy is considered to be lost due to some mechanism of friction (e.g., Kolsky, 1953; Johnston, 1979).

The tenets of the classical kinetic theory of heat (e.g., Jeans, 1940) are strikingly analogous to the OA picture: a nail heats up when hit by a hammer, for instance, because some of the ordered motions of the atoms in the approaching hammer are transformed, through unspecified mechanisms, into disordered motions of the atoms in the nail, which occur on spatial scales far below those with which the nail is observed. On observational scales, this manifests as an increase in the temperature of the nail.

If we pursue this analogy faithfully, in which the experiment, *a hammer hitting a nail*, is replaced with *a wave propagating through a medium*, and *unspecified mechanisms* are replaced with *layers with thicknesses below the seismic wavelength*, and *the temperature of the nail increases* is replaced with *the wave attenuates*, we produce a corollary to the OA view, which is that thin-bed multiples are themselves a form of heat—disordered motion occurring below the resolution of the experiment. The fact that multiples also appear in a resolvable forms in seismic data is merely an accident of the scales over which seismic sources, Earth property variations, and receivers operate.

This view is interesting because it causes the mind to focus on what is common between the mechanisms of intrinsic and scattering attenuation, as opposed to the more common tendency, which is to focus on their differences, and the beguiling idea that two such different

mechanisms could lead to the same observation.

The purpose of this paper is to investigate a way of quantifying the behaviour of seismic waves (modelled or measured) that deliberately does not distinguish between multiples and attenuation. Suppose, for instance, we were to send an elastic wave propagating past a sequence of interfaces. Suppose further that we repeated this experiment many times, each time sending in a wave with a lower central frequency. At first, the influence of the interfaces would appear as fully-resolved multiple reflections, but, as the frequency decreased, the multiples would gradually cease to be resolved, and would instead appear as amplitude and phase changes within the original wavelet. What we will derive is a measure of the wave that would respond to this progression continuously, rather than forcing us to jump from one interpretation (multiple reflections) to another (Q).

We do this by focusing on the idea of *disorder*, a word we have already used several times. We suggest that as one wave propagates through a medium that is a strong generator of multiples, and as another wave propagates through a medium that attenuates the wave, both wave fields increase in their disorder. A well-defined measure of this disorder would increase for both waves, and would not distinguish between the two.

To measure the disorder of the field we choose to calculate a version of the Shannon entropy (Shannon, 1948; Ulrych and Sacchi, 2005) defined on the spatial distribution of the wave field at a given instant of time (as if it were a random variable). We suggest that if processes of multiple reflection and processes of attenuation both contribute to the disorder of the field measured by the Shannon entropy, then waves which propagate in media capable of generating either (or both) of those phenomena should produce a time-evolution of entropy that is nondecreasing. To develop this idea, in this paper we will:

1. Derive an algorithm for estimating the Shannon entropy S of a wave field and thus its disorder;
2. Examine S for several test instances of a "wave in a box":
   (a) Case I: a wave in a homogeneous non-attenuating box;
   (b) Case II: a wave in a homogeneous attenuating box;
   (c) Case III: a wave in various heterogeneous non-attenuating boxes;

   and empirically attempt to account for the character of S as a function of t for each instance;
3. Point out relevant numerical issues in the calculation; and
4. Calculate the Shannon entropy of the Ross Lake vertical seismic profile data set, to confirm the consistency of entropy calculations involving field data with those in our synthetic experiments.

MEASURING THE DISORDER OF A WAVE FIELD

Let $u(x,t)$ be the solution of a wave equation

$$\left[\frac{\partial^2}{\partial x^2} - c^{-2}(x)\frac{\partial^2}{\partial t^2}\right] u(x,t) = 0, \tag{1}$$

We will be concerned with the distribution in space (x) of the field variable (u) for fixed times T, i.e., snapshots of the wave field $u(x,T)$. In Figure 1a and b two examples of such snapshots are illustrated. Instinctively we would probably say that (b) is more disordered than (a): the entropy measure we derive here will allow us to say this quantitatively.

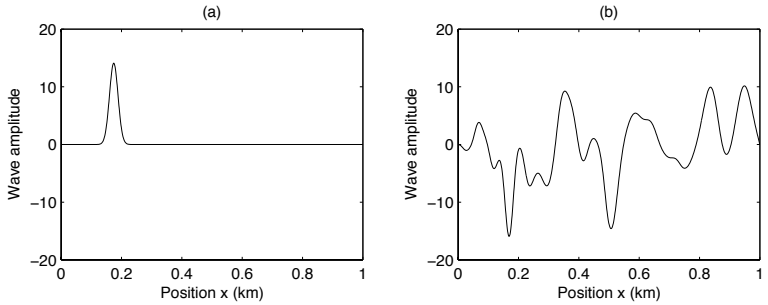

FIG. 1. Two snapshots of a wave field. Qualitatively we would call (b) more disordered, in some relative sense, than (a).

We will view these snapshots as being messages, whose information content can be measured using the Shannon entropy. To do this, we consider a discretization of space and the field u:

$$u_i(x_j,T), \quad i=(1,n), \quad j=(1,N), \tag{2}$$

The message is a "sentence" containing N "characters" (one at each point x_j). The characters are chosen from an "alphabet" of length n (one character for each possible discrete field value u_i). This is illustrated in Figure 2. In Figure 2a we have chosen the "more disordered" snapshot from Figure 1b above as an example. In Figure 2b we zoom in on a portion of the field near the halfway mark of x. In Figure 2c we illustrate the discretization: the continuous field variable u is binned into n values indexed by i, and the continuous position variable x is binned into N values indexed by j. The grey bars highlight a single "character" at the position $x_j = 0.497$km in the "sentence". The character at that position is the discrete value $u_i = -12.7$.

Suppose a random point x_j in Figure 1a was about to be chosen, and you had to bet on which associated value of u_i would come up. You would probably bet on 0, and you would probably win, because of how often 0 occurs. But if you played the same game with Figure 1b, you would be much more hard pressed: almost any value between, say -15 and +15, would seem to be equally likely. The entropy will quantify this, being large in "tough bet" situations and small in "easy bet" situations. That for us will become the measure of the order v. disorder of the wave.

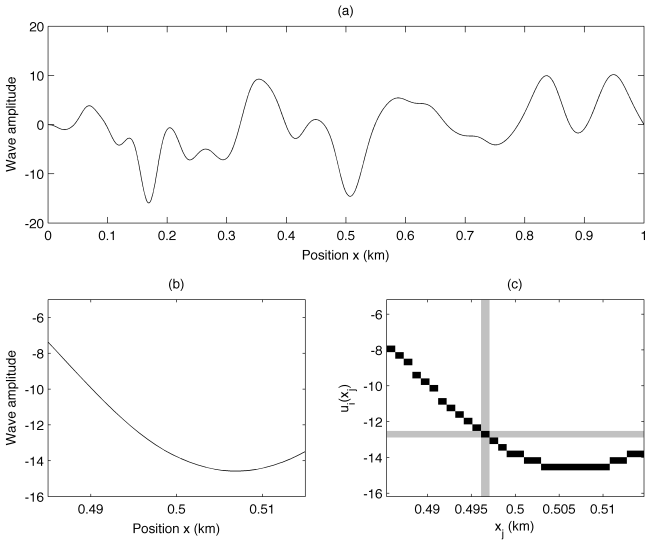

FIG. 2. Discretization of the wave snapshot. (a) Full wave field snapshot. (b) Zoom-in near the half-way point along x. (c) Discretization: vertical axis u_i, horizontal axis x_j.

For each wave field snapshot, we construct a histogram, in which the occurrences of each u_i value are enumerated:

$$W(N, i) \tag{3}$$

being the number of incidences of the wave value u_i, counted up over N position values. Histograms for the two snapshots we have been considering are illustrated in Figure 3; the histogram for the orderly wave in Figure 3a, illustrated in Figure 3b, is narrow, as most of the u_i values are 0. Whereas the histogram for the more disordered wave in Figure 3c, illustrated in Figure 3d, reflects the broader range of u_i values taken by the wave.

From these histograms we will estimate probability density functions. Since we have access to as many instances of u_i as we want or need—it is the result of our own numerical calculations—no sophisticated techniques are used. Instead, the probability p is simply the histogram, normalized:

$$p(N, i) = \frac{W(N, i)}{\sum_{k=1}^{n} W(N, k)}. \tag{4}$$

Equation (4), then, is the probability that in choosing a wave field value at random, from amongst the N values in the snapshot, you would choose the i'th value, namely u_i.

The entropy is not p itself but the result of some operations on p. To justify the particular operations, let us take a momentary excursion. In statistical mechanics W refers to the number of accessible states of a system given a certain fixed, measurable property, often the energy. Suppose for instance your system was a box containing 100 weights on springs, each of which was either oscillating with energy k, or standing still. If you measured the total energy K of the system to be $50k$, you would conclude that half of the springs were oscillating, and half were standing still. W in this case would be the number of exact

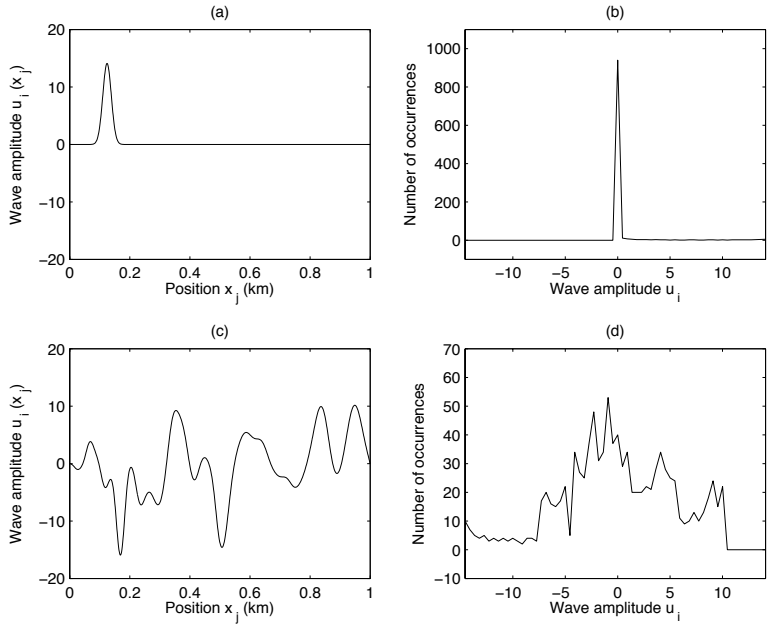

FIG. 3. Histograms of incidences of u_i. (a) The orderly wave snapshot; (b) its histogram. (c) The disorderly wave snapshot; (d) its histogram.

arrangements of the 100 weights for which 50 are oscillating, a number that happens to be $100!/[50! \times 50!] \approx 10^{29}$. A box with energy $50k$ has 10^{29} accessible states. If you measured the total kinetic energy K to be $100k$, you would conclude that all of the springs were oscillating. Since there is only one arrangement of 100 springs in which all of them are oscillating, $W = 1$ in that case. A box with with energy $100k$ has one accessible state.

By adding one more spring to the system, we double the number of its total states: (all of the originals with the new spring oscillating) + (all of the originals with the new spring standing still). This motivates the use of the logarithm to measure disorder rather than the raw distribution:

$$\log p(N, i). \tag{5}$$

Shannon in applying the idea of entropy to information used the reciprocal of p:

$$\log \frac{1}{p(N, i)} = -\log p(N, i), \tag{6}$$

on the argument that you add *more* information to a message with a new datum if that datum is *less* expected. The Shannon entropy, finally, is the average, or expectation value of equation (6):

$$S = -\sum_{i=1}^{n} p(N, i) \log p(N, i). \tag{7}$$

Since we have a p quantity expressing the arrangement of wave field values, this number $S(N)$ can be estimated for any wave field snapshot $u_i(x_j, T)$. As with any measure of entropy, the absolute value of S will likely be difficult to interpret, but its relative values may be informative. Informative about what?

THE TIME-EVOLUTION OF A WAVE IN A BOX

Our overall purpose is to develop a measure defined for a wave field that puts attenuation and multiple scattering on a roughly equal footing. That measure was defined in the previous section. It is a version of the Shannon entropy, calculated as if the wave field at a fixed time T was a random variable drawn, from a particular probability density function whose characteristics we determine from histograms.

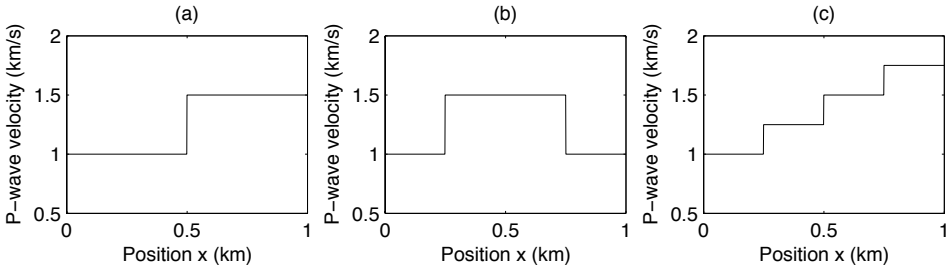

FIG. 4. Acoustic models to be studied in the context of the entropy of the evolving wave field. (a) A single interface; (b) two interfaces; (c) three interfaces. The wave will reverberate back and forth between the perfectly reflecting walls of the box, interacting repeatedly with the structures between.

What does this entropy actually measure? We will answer this question with a sequence of numerical experiments, involving a 1D scalar wave. We will make use of the same notional experiment throughout this paper: suppose we have a box with perfectly reflecting ends, containing a well defined (and choosable) set of acoustic, and/or anacoustic properties. The box has a door at one end. We excite a disturbance outside the box which propagates towards the open door, and once it passes into the box, we quickly shut the door. The wave is then trapped in the box, reverberating back and forth, either forever if the medium is acoustic, or temporarily if the medium is anacoustic. At any point after the door is shut, we will be able to measure snapshots of the wave, and these snapshots will be used to construct the functions p and thereby the number S. We will observe the evolution of the number S as the wave moves in the box.

We will consider only simple versions of this experiment, the idea being to gain basic insight. It does not, as it turns out, take a complicated medium to generate a complicated wave field. We can generate all the complexity we can handle by adding a few reflectors to the medium. The models we will study are illustrated in Figure 4), and include 1 interface, 2 interface, and 3 interface media.

Figures 5 and 6 illustrate the feel of the experiment as the wave evolves within the box, in which the three interface model has been set up. In Figures 5a–f the wave field at an early point in the evolution is illustrated. The "door" is on the left of the box, and in (a) we see the positive pulse just after its entry. The next snapshots track the wave form as it crosses the first interface, causing a reflection which propagates back to the left towards the (now closed) door.

In Figures 6a–f we return to consider the wave field after it has been propagating in the box long enough for the initial pulse to have traversed the box about 10 times. The various reflections and transmissions have by now set up a fairly complex set of oscillations, a little like a pool full of swimmers, but, tracking from (a) to (f) with the eye at roughly the same

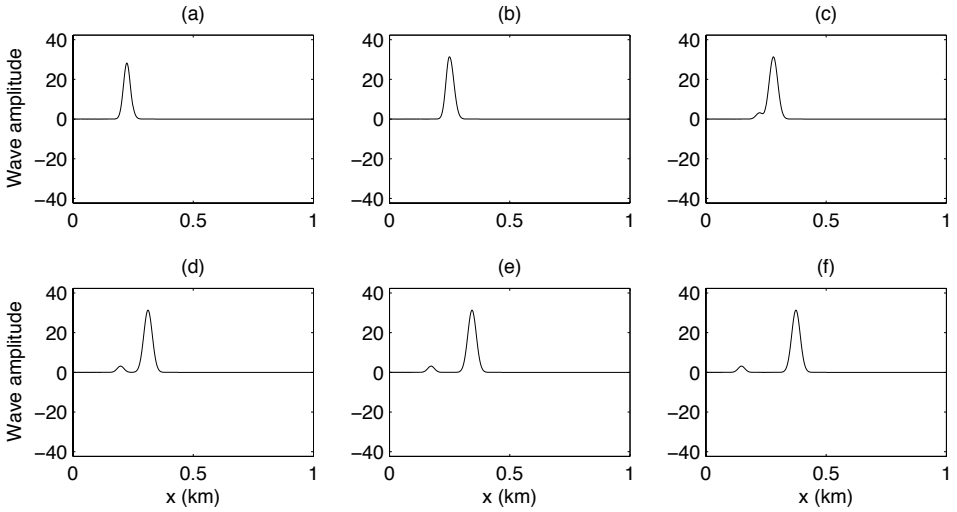

FIG. 5. Six snapshots of the wave at an early stage in its evolution. (a)–(f) the wave moves for the first time across the first of three reflectors.

locations at which the initial pulse is seen in Figures 5, the leading waveform is still visible.

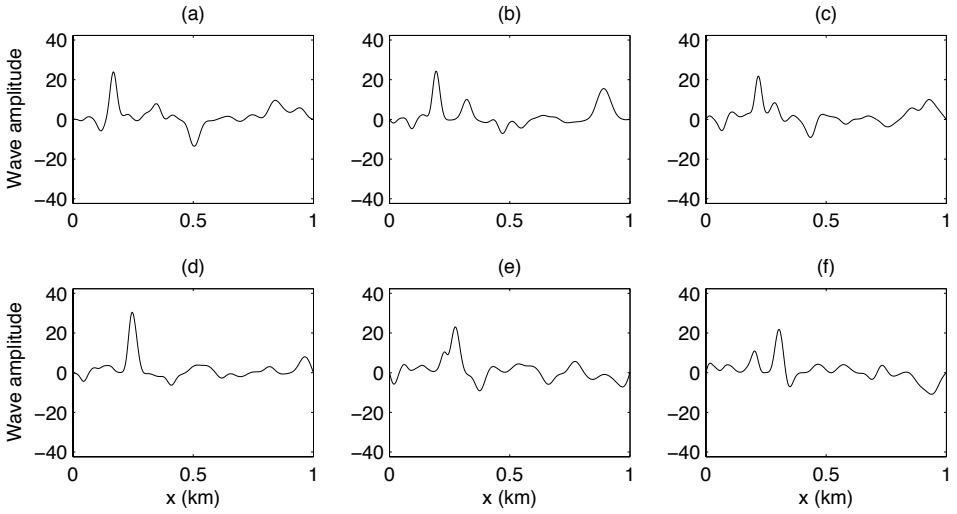

FIG. 6. Six snapshots of the wave at a later stage in its evolution. (a)–(f) the wave moves for the 10th time across the first of three reflectors.

Each of these 18 snapshots have an associated Shannon entropy. In the following sections we will repeat this wave propagation exercise, calculating and storing the associated entropy at each time point.

Case I: a homogeneous, non-attenuating medium

To establish a baseline for the entropy variations we will be trying to characterize, let us first consider the wave pulse propagating back and forth in a homogeneous medium. We will permit the wave to propagate at 1.0km/s across a box 1km in length (or equivalently at 1.0m/s across a box 1 m in length) for 5 seconds, calculating the entropy S at each time step. In Figures 7a, d, and g, we show the wave at three points during its evolution. To the left of these snapshots, in Figures 7b, e, and h, we illustrate the probability density

functions p estimated from the snapshot to the left. Since in each case the wave snapshot is simply a translation of the same wave values u_i, there is no effect on the pdf p, nor is there a change in S: in Figures 7c, f, and i the entropy S is plotted as a function of time.

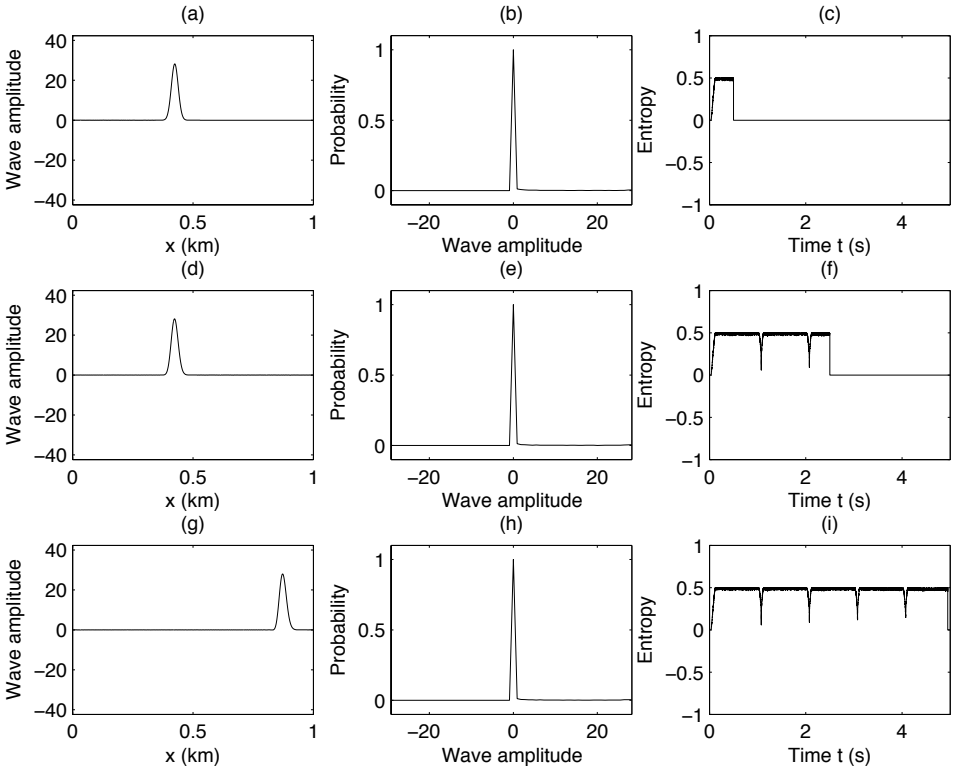

FIG. 7. The wave form $u(x,t)$, its pdf and its entropy plotted at three points during a propagation time of 5s. (a), (d), (g) Snapshots of $u(x,t)$ as a function of x at three fixed times; (b), (e), (h) the probability density functions p estimated from the waveforms to the left; (c), (f), (i) the entropy S at the time of the snapshot to the left, with

We will interpret the results of these experiments fully in the next section. However, before continuing we should address the "notches" in the time history of the entropy visible as the regularly spaced features in Figures 7c, f, and i. These are a figment of the box configuration and the wavelet width, and appear during the finite time it takes for the waveform to complete its interaction with the wall.

In Figures 8a–f we illustrate this in detail. In Figure 8a the wave is shown (moving to the left) instants before it encounters the wall. In Figure 8b the entropy at this point is plotted alongside its values over the previous several 1/100s of a second. Figures 8c-d and e-f repeat this over the duration of the interaction of the waveform with the wall. Since the wave form is reduced for a short time to essentially zero, during which time the pdf and the entropy also fall to zero, a notch appears and then disappears as the wave returns moving in the opposite direction.

Though interesting in its own right, we will consider this notching to be a sort of footprint, which we will look beyond for the evolutionary characteristics of S which shed light on the complexity of the wave.

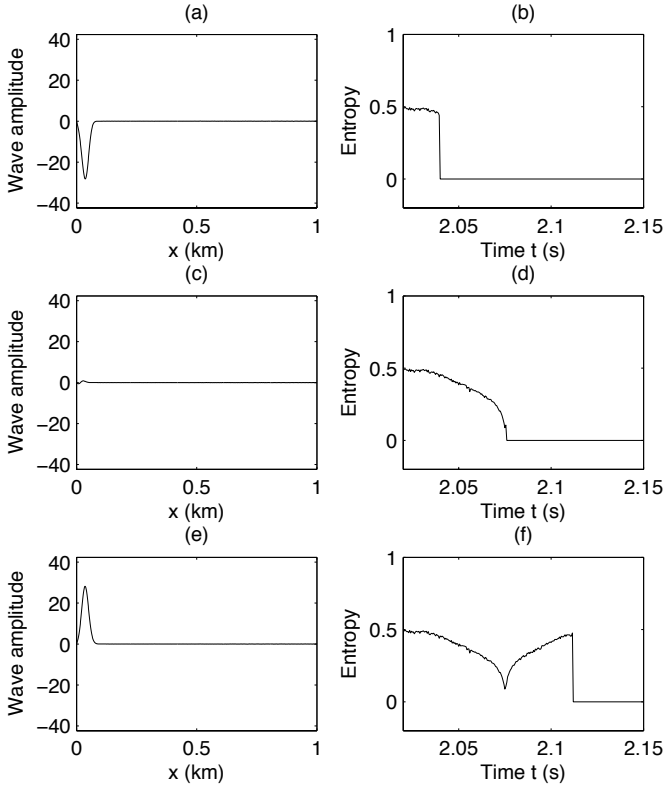

FIG. 8. Illustration of the notching in S associated with the interaction of the wave with the box walls. (a), (c), (e) Snapshots of the wave before, during and after reflection from the left-hand wall of the box; (b), (d), (f) the resultant decrease and increase of the entropy S.

Case II: a homogeneous, attenuating medium

Next we consider propagation in a homogeneous medium which is attenuating, i.e., in which the wave propagates with a fixed reference phase velocity and a fixed quality factor Q. We will hold the fixed velocity at 1.0km/s, and permit the wave to propagate the length of the box three times, each time with a decreasing quality factor.

In Figure 9 the first of these experiments is summarized. A relatively high Q factor of 200 is used. In the left column, Figures 9a, d, and g, the wave field snapshots are illustrated. By (g) some minimal amount of attenuation is visible. The pdfs are plotted in the middle column (b, e, and h), and the time-history of the entropy S is plotted in the right column (c, f, and i). The entropy shows a slow growth over time.

In Figure 10 we summarize the second run, for which the Q value is dropped to 50. The entropy evolves in much the same way, but grows more rapidly.

Finally in Figure 11 we summarize the third run, for which the Q value has been further reduced, to 20. Again the entropy S grows, with a larger growth rate and larger final value.

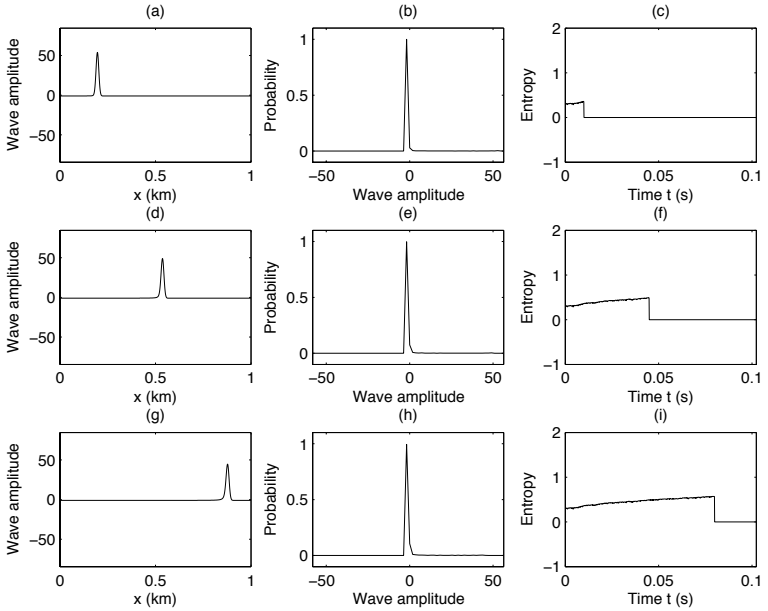

FIG. 9. Wave in a homogeneous attenuating medium with $Q = 200$. (a), (d), and (g) Snapshots of the field at early, middle and late times; (b), (e), and (h) the pdfs derived from the waveform snapshots; (c), (f), and (i) the time history of the entropy S.

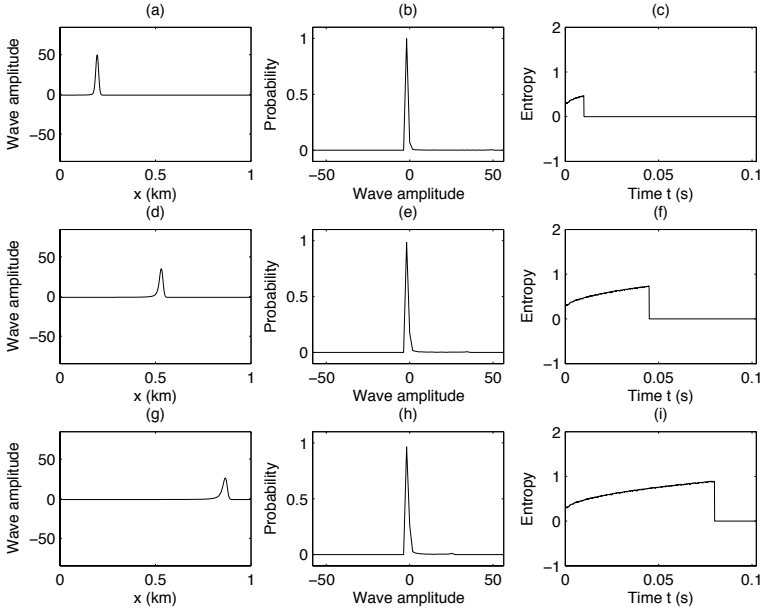

FIG. 10. Wave in a homogeneous attenuating medium with $Q = 50$. (a), (d), and (g) Snapshots of the field at early, middle and late times; (b), (e), and (h) the pdfs derived from the waveform snapshots; (c), (f), and (i) the time history of the entropy S.

Case III: a heterogeneous, non-attenuating medium

In this section we will continue our survey of the time-evolution of the Shannon entropy of a wave in a box. In this set of experiments, the medium will lose its ability to attenuate the wave—the wave field in the box, if left alone, will oscillate with the same overall energy forever. The entropy, however, which is sensitive to the distribution of the energy in the waveform, will change with time, and our interest will be to understand how it changes.

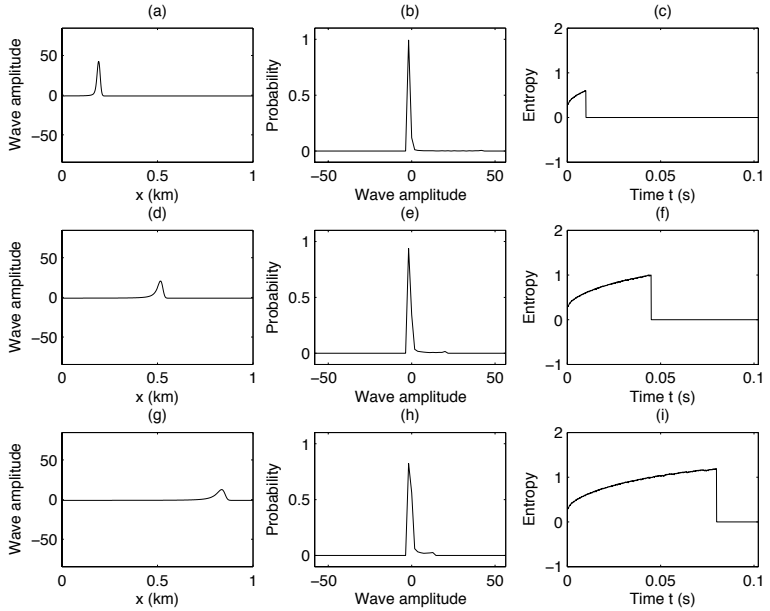

FIG. 11. Wave in a homogeneous attenuating medium with $Q = 20$. (a), (d), and (g) Snapshots of the field at early, middle and late times; (b), (e), and (h) the pdfs derived from the waveform snapshots; (c), (f), and (i) the time history of the entropy S.

i. One interface

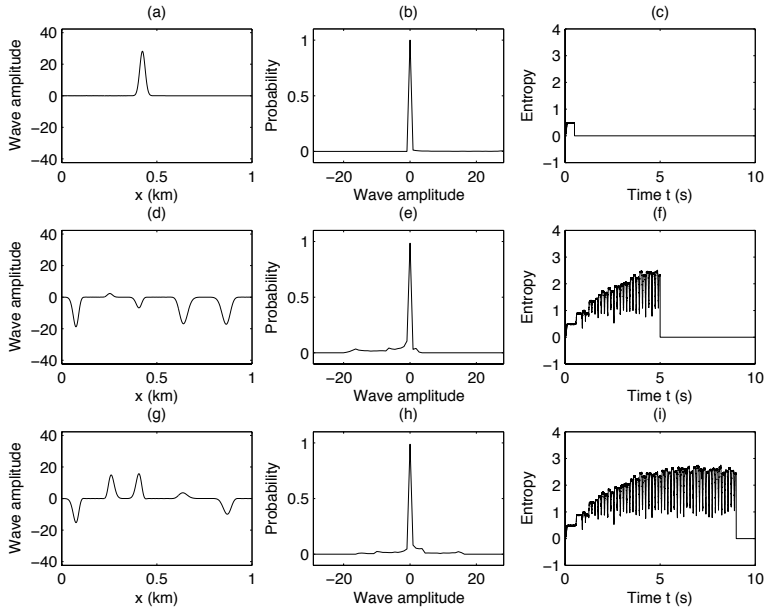

FIG. 12. Wave field snapshots and Shannon entropy for the one interface medium. The wave begins at the left wall of the box, and interacts with the velocity model depicted in Figure 4a. (a), (d), (g) Snapshots of the wave; (b), (e), (h) the estimated pdfs; (c), (f), (i) the time evolution of the Shannon entropy.

We begin with the single interface model in Figure 4a. The initial wave field, a right-propagating Gaussian function with a variance and amplitude chosen such that the integral of the wave field is 1, begins at the left end of the box. It encounters the single boundary, reflects and transmits. Both of these wave components continue to opposite walls of the

box, reflect, and return again to encounter the boundary. At each encounter, the energy of the wave is re-partitioned, potentially influencing S. This is illustrated with three wave snapshots in Figure 12.

ii. Two interfaces

We next repeat the exercise with the two interface model depicted in Figure 4b. The idea is the same—the partitioning of wave energy at the interfaces causing the distribution of wave field u values and thus altering the Shannon entropy S as we calculate it using equation (7). The only difference is that there are now two rather than one interfaces—twice as many opportunities for the disorder of the wave to increase. The results are summarized in Figure 13.

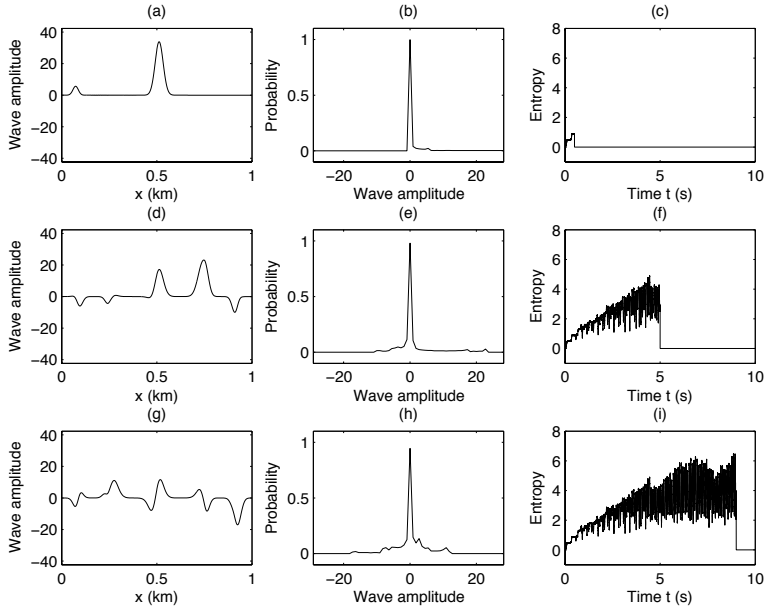

FIG. 13. Wave field snapshots and Shannon entropy for the two interface medium. The wave begins at the left wall of the box, and interacts with the velocity model depicted in Figure 4b. (a), (d), (g) Snapshots of the wave; (b), (e), (h) the estimated pdfs; (c), (f), (i) the time evolution of the Shannon entropy.

iii. Three interfaces

We then again repeat the experiment for the three interface model illustrated in Figure 4c. The results are summarized in Figure 14.

Numerical issues in entropy estimation

All of the numerical examples so far have been calculated with identically-sized histograms, with 64 bins of the same width, spanning amplitudes ranging from the maximum to the minimum amplitude taken on by the wave. There is a sensitivity of the calculation to the bin number, however; in this section we will point out what we believe are the two key details associated with that choice.

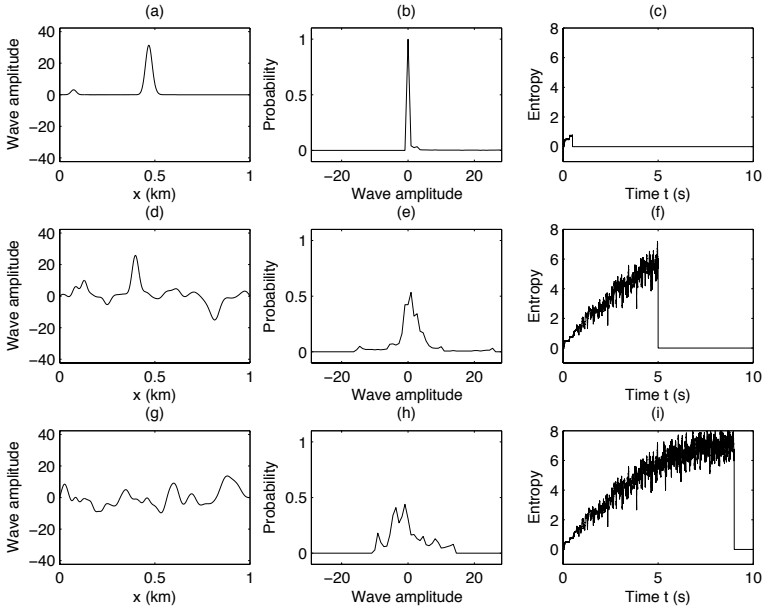

FIG. 14. Wave field snapshots and Shannon entropy for the two interface medium. The wave begins at the left wall of the box, and interacts with the velocity model depicted in Figure 4b. (a), (d), (g) Snapshots of the wave; (b), (e), (h) the estimated pdfs; (c), (f), (i) the time evolution of the Shannon entropy.

First, the entropy calculation done with one bin size (say 2^N) and another (say 2^M) should be scaled prior to comparison, by a factor 2^{M-N}. In Figure 15a-b, for instance, the homogeneous attenuating problem (with $Q = 20$) is calculated twice, once with a bin size of 64 (black) and again with a bin size of 256 (red). The two are comparable, since the latter has been corrected by a factor of $2^{7-5} = 4$. While there is some difference, at early times the two calculations of S track well.

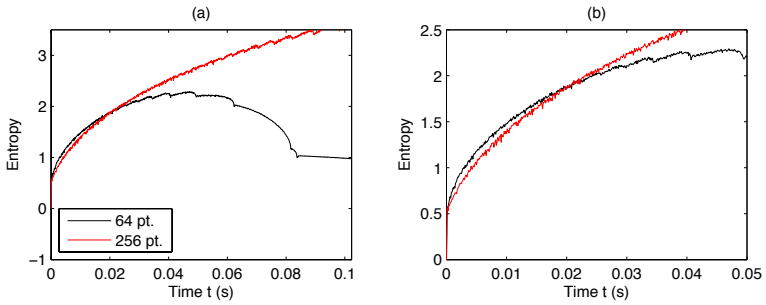

FIG. 15. The time evolution of a wave in a homogeneous, attenuating box with $Q = 20$ using two different histogram bin sizes. (a) In red is the entropy calculated with 256 bins, in black the entropy calculated with 64 bins, with the former scaled by 2^2 before comparison to the latter. (b) Zoomed in version of (a).

The second key issue has to do with the differences visible in Figure 15a at later times, wherein the S calculation for a smaller bin size begins to decay, ultimately falling to a hard zero. This is in distinct contrast to the non-attenuating case over long times, wherein a state of equilibrium is attained and kept perpetually (see Figure 16, in which the 2-interface, non attenuating Shannon entropy is illustrated for a relatively long integration time). As the wave attenuates, the entropy of the wave, in the sense of its disorder, does increase, but the decay of the amplitudes gradually makes a given choice of bin size improper, and skews

the calculation downward. Regardless of how liberally the amplitudes are distributed, if they fall are all adjudged to fall into the "zero" bin, the resulting S will be close to zero. It is important to bear in mind that this is a numerical artifact (unavoidable in any numerical estimation of S), which carries little information about the physical process.

We recommend (1) a choice of bin size which maintains the non-decreasing nature of S with integration time, (2) a favouring of early times in the evolution of S for its characterization, and (3) if S values calculated with different bin sizes/numbers are to be compared, they be scaled to account for this difference first.

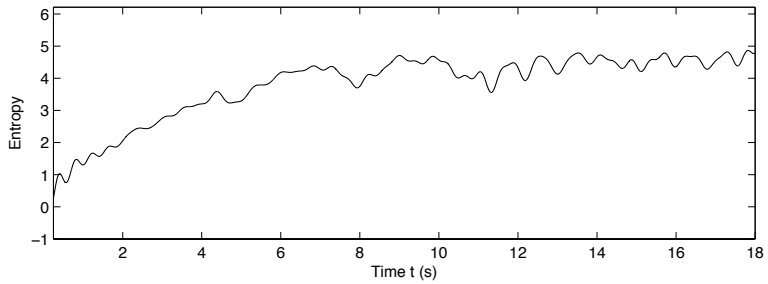

FIG. 16. The time evolution of a wave in a heterogeneous, nonattenuating box (two interface case). A long integration time are illustrated.

Summary: the ability of Q and heterogeneity to create disorder

The heterogeneous, non-attenuating examples appear to have tended to successfully generate "disordered" fields, in the sense of our earlier remarks. Further, our Shannon entropy S does increase as disorder (at least, our qualitative sense of it) increases. There are a number of observations which seem to hold true for all examples:

1. S remains constant for wave forms propagating in homogeneous regions of a model.
2. Although it experiences fluctuations (generally caused by the notching behaviour discussed earlier), in general S is a nondecreasing function of time.

Let us compare the disorder generated in the wave field due to acoustic heterogeneous media vs. that generated in the wave field due to attentive homogeneous media.

Disorder from intrinsic attenuation

In Figure 17 we examine the change in the time evolution of the entropy S for a wave propagating through media with gradually decreasing Q values. A distinctive trend emerges: as Q decreases (i.e., attenuation increases), a greater final value of S is attained in a shorter time. S traces out a curve reminiscent of a semivariance plot, with common nugget but larger sill values as $Q \rightarrow 0$.

Hence attenuation has a marked ability to increase the disorder of the wave field, which (to the extent it is measured by the Shannon entropy S) increases systematically as the medium Q value decreases. The disorder is created by the attenuation and dispersion:

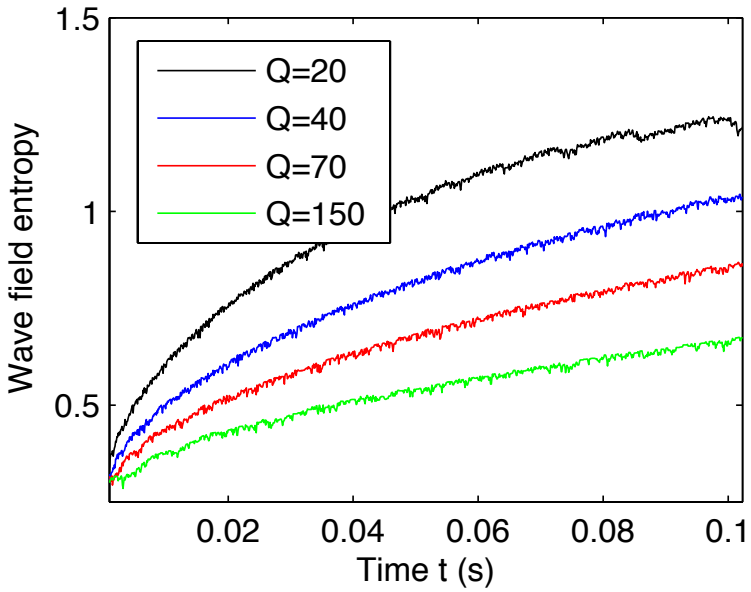

FIG. 17. The ability of homogeneous, attenuating media to alter the Shannon entropy S. The same experiment is repeated for four different Q values.

a pulse which is "spike-like", and thus contains relatively few wave elements with large values, is smoothed out in such a way that in the histograms used to calculate S, a larger number of discrete bins contain a larger number of instances.

Disorder from heterogeneity

A homogeneous attenuating medium causes the wave field to become increasingly disordered as it propagates. We see similar behaviour in the time evolution of S in heterogeneous media, with a *growing number of interfaces* playing a similar role to the one a *decreasing Q value* did in the previous section. See Figure 18a–b, the latter panel of which has been filtered to emphasize the trend. The difference between the two is in the time- and amplitude scales of the phenomena—the multiple acoustic interfaces generate a larger entropy, following a similar trend which recalls semivariance, but it does so over a longer time-scale.

Every time a wave strikes a boundary in the box model, the entropy has the capacity to grow. At early stages in the propagation, this possibility for growth is almost always realized, because, if the wave energy is distributed in a very orderly way at the outset, almost any re-distribution of the energy (for instance after a reflection) will correspond to a larger number of accessible states for the wave field to take on. So, early on, the entropy grows rapidly.

As the wave energy is more liberally spread out through the box, interactions with the interfaces can lead to small or even zero increases in S. This is because a wave going in one direction past a boundary can have reflected and transmitted components which "scattering into" transmitted and reflected components which were simultaneously incident on the boundary from the other direction, leaving the overall distribution of wave energy

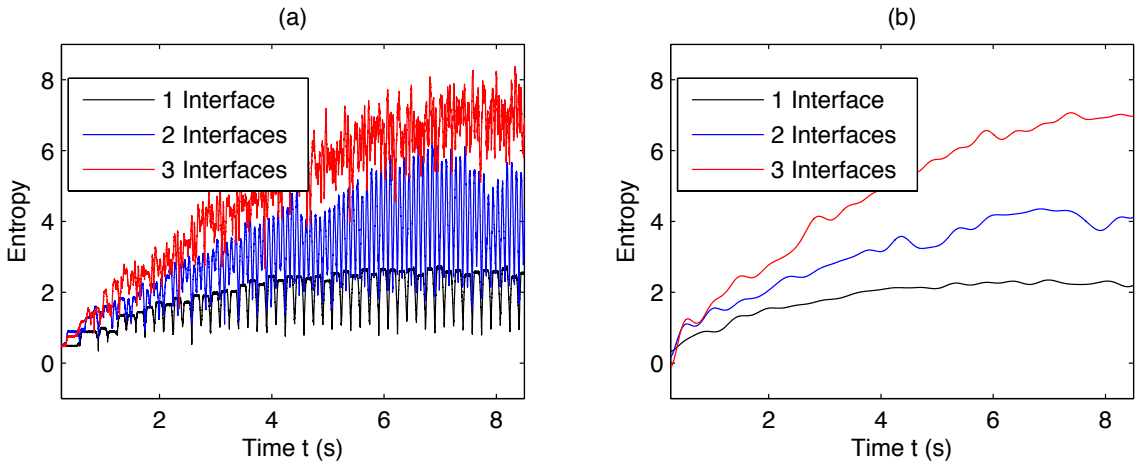

FIG. 18. The ability of heterogeneous, non attenuating media to alter the Shannon entropy S. (a) S as a function of time compared for media with one (black), two (blue) and three (red) interfaces. (b) The same curves filtered to enhance the trend.

in the box unchanged, or nearly unchanged. As the wave disorder increases this becomes more and more likely, gradually becoming more likely than an actual increase in S. Thus with the exception of fluctuations, S ceases growth at a certain time.

Remark

The Shannon entropy of a propagating wave evidently undergoes changes with time which are qualitatively similar regardless of whether the dominant process at work is multiple reflection, or attenuation.

THE SHANNON ENTROPY OF A FIELD VSP DATA SET

This is a paper principally about how to define measures on seismic waves which view attenuation and multiple scattering as indistinct. It is not intended to advocate the Shannon entropy as a particular means to estimate Q, though it might have value in that arena in the future. In spite of this, it would be valuable to confirm that actual observations of seismic motions behaved in some sense as we have discussed above.

Able as it is to provide wave field measurements with both extent in both time and position (in the direction of propagation), a VSP survey is an ideal setting in which to test Shannon entropy calculations on seismic observations. The Ross Lake VSP data set (Haase and Stewart, 2006) has the additional benefit of having been shown independently to involve significant levels of attenuation. In Figure 19a the zero offset component of the full walkaway survey is illustrated; in Figures 19b–d we focus on traces for an increasing range of depths, illustrating visually the attenuation of the direct wave.

The VSP data set permits us to make a “movie” of the wave during propagation, by drawing a horizontal line across the top of Figure 19a, and letting the line sweep downward. The wave field at each time point can be used to estimate the distribution of wave amplitudes, and thereafter the Shannon entropy S. Doing so for each time point allows

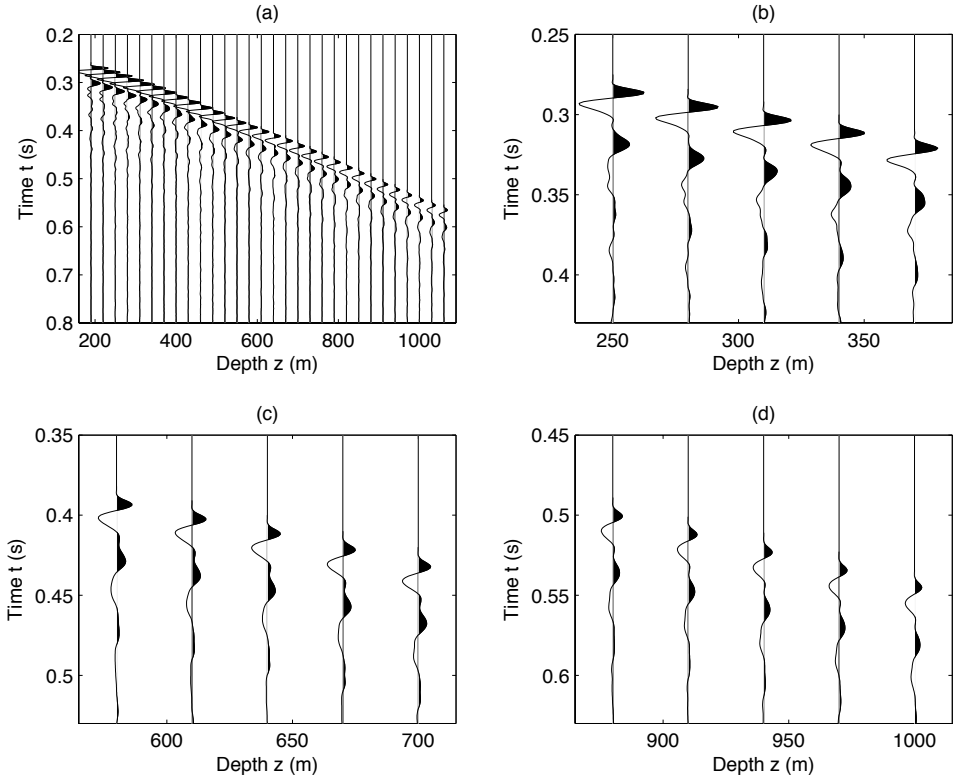

FIG. 19. The zero offset component of the Ross Lake VSP data set. (a) All depths; (b)–(d) zoomed in regions to illustrate progressive attenuation.

us to form a time-evolution of S just like those we have investigated with synthetic waves previously. In Figures 20a-b the time evolution of S is plotted four times, each time using a different bin size. The values of S are scaled as per the earlier recommendations. The expected decay of S at later times, especially for the large bin sizes (i.e., smaller number of bins), is confirmed in the field data by the red and blue curves, . This being an artifact, we prefer to focus on the smaller bin size in green and black, which are in agreement about the magnitude and rate of growth of the Ross Lake entropy for most of the duration that the direct wave remains in the data.

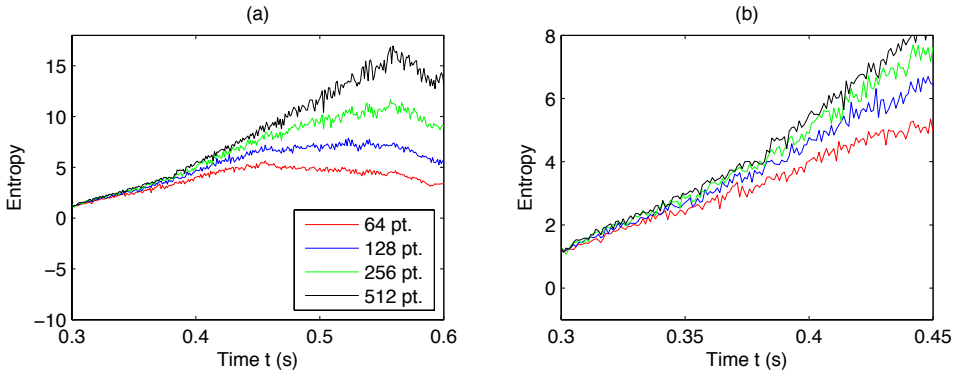

FIG. 20. The Shannon entropy of the zero offset Ross Lake data. (a) S calculated using four different bin lengths and sizes for the full time history in which the direct wave is detected in the VSP data; (b) zoom in on early times.

We conclude that the behaviour of the Shannon entropy as deduced from synthetic experiments is in essential agreement with field VSP data through attenuating geological structures.

CONCLUSIONS

Both attenuation and multiple scattering have the same effect on the time evolution of the Shannon entropy (as calculated on the instantaneous spatial distribution of wave disturbance). The reason is that under this model, a process like reflection at a boundary is seen to increase the bulk disorder of the field, as is the spreading out of amplitudes occurring in anelastic propagation.

As a consequence, the entropy measure tends to blur the distinction between the two most often discussed origins of seismic amplitude losses, namely intrinsic and extrinsic attenuation. For instance, consider a wave propagating past a sequence of elastic interfaces. Further, consider that we have the capacity to repeat this experiment with a pulse with a progressively decreasing central frequency. At first, the influence of the interfaces would be felt as fully-resolved multiple reflections, but as the frequency decreased, the multiples would gradually cease to be resolved, and would instead appear as amplitude and phase changes within the original wavelet.

We have developed a means of discussing the progression through this set of experiments in terms of a continuous quantity, an adapted version of the Shannon entropy. It, in fact, provides as a limiting case a working definition of what we might mean by "truly" intrinsic attenuation: disordered elastic motion occurring on spatial scales small enough that they are observed as an increase in the temperature of the medium.

The Shannon entropy is a number that is easily computable from measurements of seismic data, as we have shown both synthetically and with a field VSP data set. There are numerical issues, of course, and a consistent calculation will ultimately have to be based on solid estimates of wave field histograms and probability density functions; we may not yet have attained that.

ACKNOWLEDGMENTS

This work was funded by the CREWES project. CREWES sponsors and research personnel are thanked.

REFERENCES

Haase, A. B., and Stewart, R. R., 2006, Intrinsic and apparent attenuation in VSP data: SEG Expanded Abstracts, **25**, 3472–3476.

Jeans, J., 1940, An introduction to the kinetic theory of gases: Cambridge University Press.

Johnston, D. H., 1979, Attenuation: a state of the srt summary: In: Seismic Wave Attenuation, Toksöz and Johnston, Eds., 123–135.

Kolsky, H., 1953, Stress waves in solids: Oxford University Press, 1st edn.

O'Doherty, R. F., and Anstey, N. A., 1971, Reflections on amplitudes: Geophysical Prospecting, **19**, 430–458.

Shannon, C. E., 1948, A mathematical theory of communications: Bell System Technical Journal, **27**, 379–423,623–656.

Ulrych, T. J., and Sacchi, M. D., 2005, Information-based inversion and processing with applications: In: Handbook of geophysical exploration: seismic exploration, Elsevier, K. Helbig and S. Treitel Eds., 405.